Peter Jäckel*

Hyperbolic local volatility

First version: 13th November 2006
This version: 12th December 2008

Abstract

A parametric local volatility form based on a hyperbolic conic section is introduced, and details are given as to how this alternative local volatility form can be used as a drop-in replacement for the popular Constant Elasticity of Variance local volatility model [Cox75, Bec80], and what parameter restrictions apply.

1 Introduction

The Constant Elasticity of Variance (CEV) model is a well-known way to parametrise the dependence of absolute instantaneous volatility on movements of an underlying financial observable S:

$$\sigma_{\text{CEV, absolute}} \;=\; \sigma_{\text{CEV}} \cdot S^{\beta} \tag{1}$$

As a stochastic process, the CEV model is often described by the differential equation

$$\mathrm{d}S \;=\; \sigma_{\text{CEV}} S^{\beta} \mathrm{d}W \;, \tag{2}$$

with $\mathrm{d}W$ standing for the infinitesimal increment of a standard Wiener process. This stochastic differential equation allows for closed form solutions for the prices of plain vanilla options [Cox75, Sch89] which is one of the reasons for its popularity. Equivalent Black volatilities can be implied from vanilla option prices for different strikes, allowing the use of β as a parameter to match the market-observable *skew* for vanilla options. Values for β less than one, for example, give a negative skew as often observed in equity and interest rate markets.

Alas, the CEV model doesn't only have advantages. It also brings with it a range of problems:

- Its vanilla option formula depends either on the approximation of an infinite series of Gamma functions or on the evaluation of the non-central chi-squared distribution function, "which is notoriously difficult to compute quickly and accurately" [NN05].
- Numerical evaluations based on finite difference methods as well as Monte Carlo simulations incur difficulty near $S = 0$. The problems near zero arise because no simple transformation can be invoked to enable valuation on a homogeneous scale because, near zero, Itô's lemma does not hold for any function $f(S)$ if S is governed by (2) for $\beta < 1$. The problems are so serious that, for practical applications, some authors have suggested to suppress the CEV scaling behaviour altogether near zero, and to assume a piecewise linear (and thus manageable) form in a small neighbourhood of zero instead [AA00].

*OTC Analytics

- The β parameter values required to match market-observable implied volatility skews are often near zero, and always less than 1. As a consequence, implied volatilities for high strikes, become very small. In fact, with increasing strike, implied volatility even converges to zero!
- For market-calibrated values of β, the process (2) can attain zero. This not only adds to the numerical inconveniences, but also means that any financial product whose value becomes undefined when zero is attained cannot be priced with a CEV model.

A common approximation for the CEV model to overcome the difficulty with analytical formulae and numerical schemes near zero is to replace (2) with the displaced diffusion model [Rub83]

$$\mathrm{d}S \;=\; \sigma_{\text{DD}}\,[\beta S + (1-\beta)S_0]\,\mathrm{d}W\;. \tag{3}$$

This has the advantage that plain vanilla options can be valued with a call to the Black function with modified inputs, and thus become reliable to evaluate. Stable numerical schemes can also be designed based on the transformation

$$S \;\rightarrow\; \tilde{S} = \beta S + (1-\beta)S_0\;. \tag{4}$$

since $\tilde{S}$ is lognormal under (3). Also, implied volatility for high strikes for the displaced diffusion model converges to $\sigma_{\text{DD}}\beta$ and not to zero. However, the displaced diffusion model for $\beta < 0$ still allows zero to be attained, even negative values for S are possible!

Inspired by the affine functional form for absolute volatility of the displaced diffusion model (3), we seek an alternative replacement for the CEV model that retains the advantage that implied volatility for high strikes does not converge to zero, and is numerically smooth to handle. In addition, however, we also wish to avoid zero being an attainable boundary, as well as analytical behaviour near zero. We are prepared to give up exact analytical tractability of plain vanilla option prices, though, as long as we can find sufficiently accurate approximations that are easy to evaluate.

In the following, we always assume that any parametric local volatility model given by a stochastic differential equation of the form

$$\mathrm{d}S \;=\; \sigma_S \cdot f(S) \cdot \mathrm{d}W \tag{5}$$

is transformed both in variables and parameters according to

$$\begin{aligned}
\sigma \;&:=\; \sigma_S f(S_0)/\,S_0 && (6)\\
x \;&:=\; S/\,S_0 && (7)\\
x_0 \;&=1 && (8)\\
\zeta(x) \;&:=\; f(x\cdot S_0)/\,f(S_0) && (9)
\end{aligned}$$

such that

$$\mathrm{d}x \;=\; \sigma \cdot \zeta(x) \cdot \mathrm{d}W \tag{10}$$

with $\zeta(x_0) = \zeta(1) = 1$. In short, we seek a function $\zeta(x)$ that can be used as a drop-in replacement for x^β.

2 Hyperbolic local volatility

A hyperbola can be described by the implicit equation

$$\left(\frac{x}{a}\right)^2 - \left(\frac{y}{b}\right)^2 \;=\; 1 \tag{11}$$

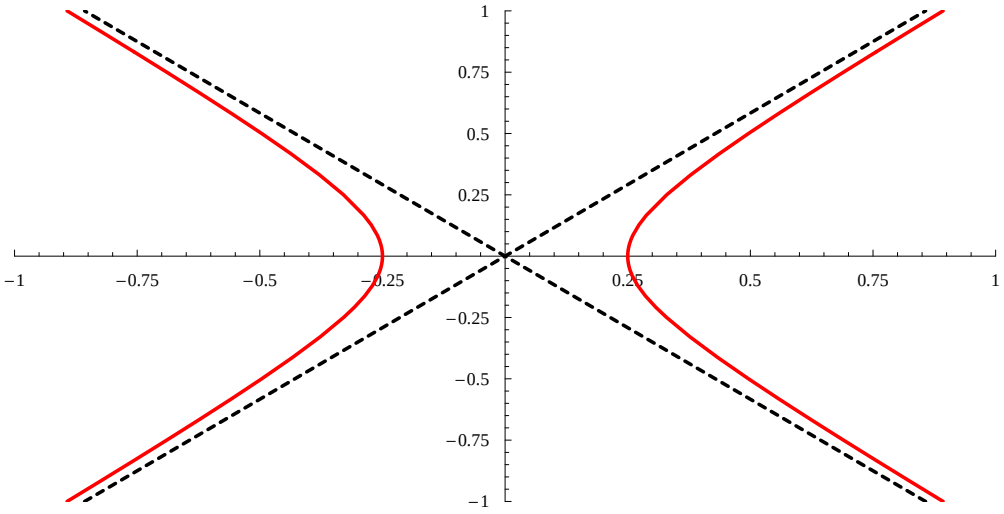

Figure 1: A standard hyperbola with $a = 1/4$ and $b = 7/24$.

For any given a and b, all points (x, y) that satisfy (11) form the hyperbola of *semi-major axis length* a and *semi-minor axis length* b. Note that b can be larger than a (in fact, for our applications, we want it to be as we shall see later). A standard hyperbola is shown in figure 1. Since the ratio of y to x, for large x, converges to b/a, a standard hyperbola has an opening angle greater than 90 degrees when $b > a$, which is a condition we from now on impose. Rotating the same hyperbola by 45 degrees in a clockwise direction, results in the curve shown in figure 2. Adding an offset to the coordinate system

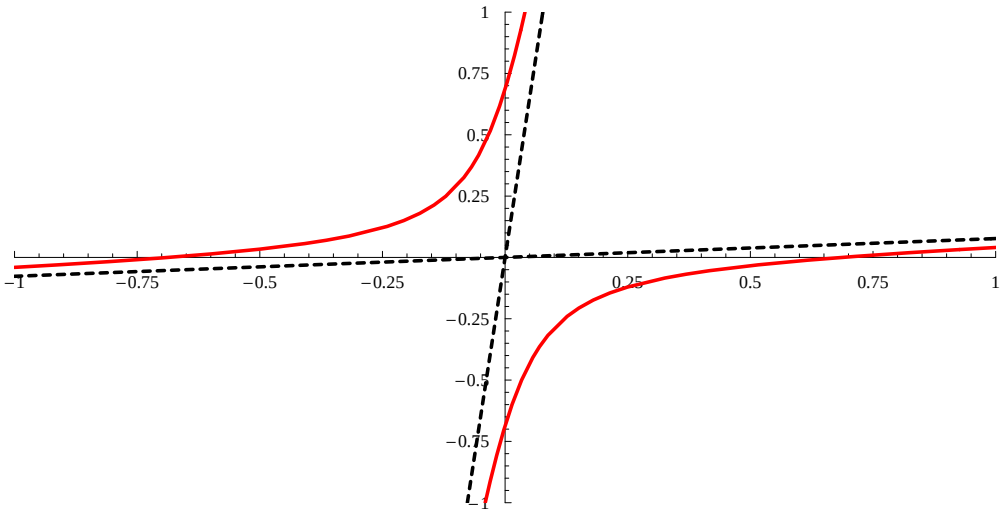

Figure 2: A hyperbola with $a = 1/4$ and $b = 7/24$, rotated clockwise by $\pi/4$, i.e. 45 degrees.

means we now look at the coordinates given by

$$\begin{pmatrix} \tilde{x} \\ \tilde{y} \end{pmatrix} = \frac{1}{\sqrt{2}} \begin{pmatrix} 1 & 1 \\ -1 & 1 \end{pmatrix} \cdot \begin{pmatrix} x \\ y \end{pmatrix} + \begin{pmatrix} x_0 \\ y_0 \end{pmatrix} \tag{12}$$

with (x, y) still satisfying (11). For $b > a$, it is possible to find (x_0, y_0) such that the lower branch of the rotated and shifted hyperbola always goes through both $(\tilde{x}, \tilde{y}) = (0, 0)$ and $(\tilde{x}, \tilde{y}) = (1, 1)$. This solution is given by:

$$x_0 = \frac{1}{2} - \frac{1}{2}\frac{a}{b}\sqrt{1 + 2b^2} \tag{13}$$

$$y_0 = \frac{1}{2} + \frac{1}{2}\frac{a}{b}\sqrt{1 + 2b^2} \tag{14}$$

In our graphical example, this results in the hyperbolic form shown in figure 3. The full functional

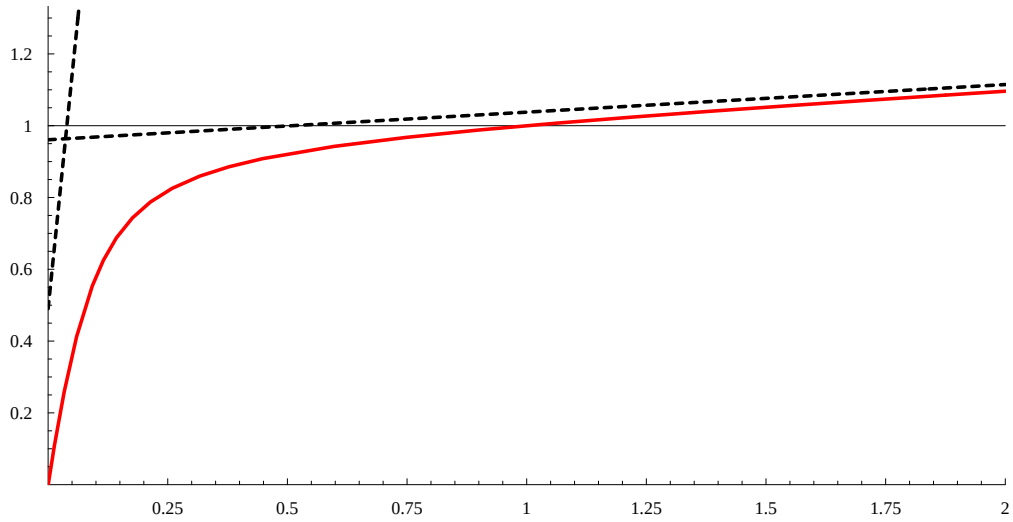

Figure 3: A hyperbola with $a = 1/4$ and $b = 7/24$, rotated clockwise by $\pi/4$, i.e. 45 degrees, and shifted such that it goes through the points $(0, 0)$ and $(1, 1)$.

form for this hyperbolic conic section is $\tilde{y} = h(\tilde{x}; a, b)$ with

$$h(x; a, b) = \frac{a^2 - (a^2 + b^2)x - ab\sqrt{1 + 2b^2} + a\sqrt{a^2 + b^2(2b^2 + (1 - 2x)^2) - 2ab(1 - 2x)\sqrt{1 + 2b^2}}}{a^2 - b^2} \,. \tag{15}$$

By construction, the function $h(x; a, b)$ satisfies $h(1; a, b) = 1$ for all $a > 0$ and $b > a$. Also, by virtue of being a segment of a hyperbolic form, it always has finite slope as $x \to 0$ which suffices for S not being able to attain zero if we use $h(x; a, b)$ as a normalised local volatility function $\zeta(x)$. In fact, it is straightforward to prove the reciprocal relationship

$$\left.\frac{\partial h(x; a, b)}{\partial x}\right|_{x=0} = \left(\left.\frac{\partial h(x; a, b)}{\partial x}\right|_{x=1}\right)^{-1} \tag{16}$$

and since the slope of $h(x; a, b)$ at $x = 1$ is finite, its reciprocal value, which is the value of the slope at $x = 0$, must also be finite.

The hyperbolic form (15) has two free parameters, namely a, and b, with the restrictions $b > a$ and $a > 0$. We can use these to match the CEV local volatility function x^β in some sense. The first criterion for a functional similarity, apart from going through $(0, 0)$ and $(1, 1)$, and having unlimited growth for $x \to \infty$, that springs to mind, is local similarity near 1. For this purpose, for any given value for β, we wish to find a and b such that

$$\left.\frac{\partial h(x; a, b)}{\partial x}\right|_{x=1} = \left.\frac{\mathrm{d}x^\beta}{\mathrm{d}x}\right|_{x=1} \tag{17}$$

which equates to

$$\frac{b\sqrt{1 + 2b^2} - a}{b\sqrt{1 + 2b^2} + a} = \beta \,. \tag{18}$$

An intuitive choice for a second condition to pin down both a and b is

$$\left.\frac{\partial^2 h(x; a, b)}{\partial x^2}\right|_{x=1} = \left.\frac{\mathrm{d}^2 x^\beta}{\mathrm{d}x^2}\right|_{x=1} \tag{19}$$

which translates into

$$\frac{-8ab^4}{(b\sqrt{1+2b^2}+a)^3} \;=\; \beta(\beta-1)\;. \tag{20}$$

Equations (19) and (20) have the solution

$$a \;=\; \left(\tfrac{1-\beta}{1+\beta^2}\right)\cdot\sqrt{\beta} \qquad\qquad b \;=\; \sqrt{\tfrac{\beta}{1+\beta^2}}\;. \tag{21}$$

This gives us the simpler form for (15) which is now matched to the CEV form x^β in both slope and curvature at $x = 1$:

$$h(x) \;=\; \frac{1-\beta+\beta^2}{\beta}\cdot x + \frac{\beta-1}{\beta}\cdot\left(\sqrt{x^2+\beta^2(1-x)^2}-\beta\right)\;. \tag{22}$$

The three functional forms (2), (3), and (22) are shown in figures 4 and 5. Since the limiting behaviour

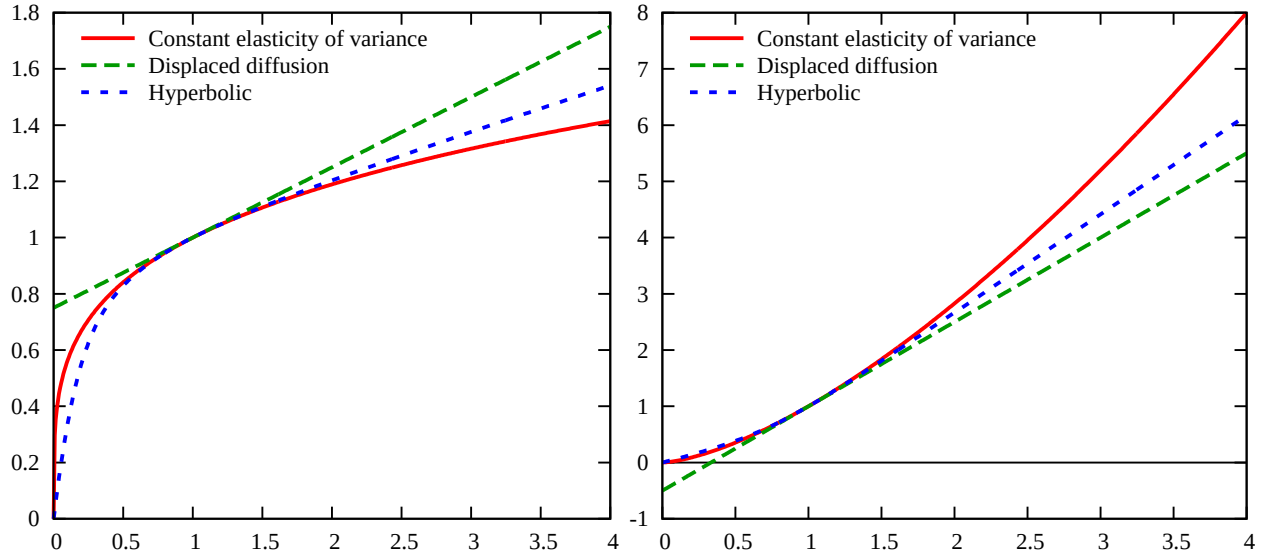

Figure 4: Absolute volatility for constant elasticity of variance (red, solid), displaced diffusion (green, long dashes), and hyperbolic (blue, short dashes) local volatility forms for $\beta = 1/4$ (left) and $\beta = 3/2$ (right).

of implied Black volatilities as a function of strike for time-homogeneous local volatility models is given by the limiting behaviour of *relative* local volatility [BBF02], we have immediately

$$\lim_{K\to\infty}\hat{\sigma}_{\text{hyperbolic}}(K) \;=\; \beta - 1 + \sqrt{1+\beta^2} + \left(1-\sqrt{1+\beta^2}\right)\Big/\,\beta \tag{23}$$

$$\lim_{K\to 0}\hat{\sigma}_{\text{hyperbolic}}(K) \;=\; 1/\,\beta\;. \tag{24}$$

The functional forms (23) and (24) are shown in figure 6.

3 Analytical approximations

It can be shown generically by the aid of asymptotic expansion techniques [Wat87, Kah07] that the equivalent Black implied volatility $\hat{\sigma}$ for options struck at $1+\xi$ for an underlying whose dynamics

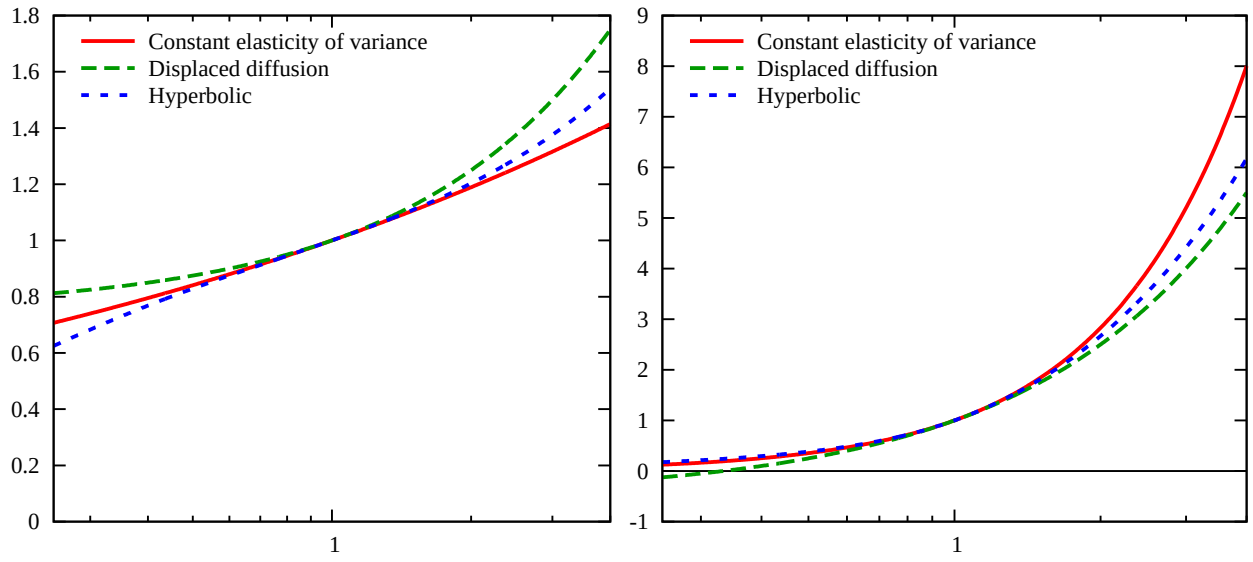

Figure 5: Absolute volatility on a logarithmic scale for constant elasticity of variance (red, solid), displaced diffusion (green, long dashes), and hyperbolic (blue, short dashes) local volatility forms for $\beta = 1/4$ (left) and $\beta = 3/2$ (right).

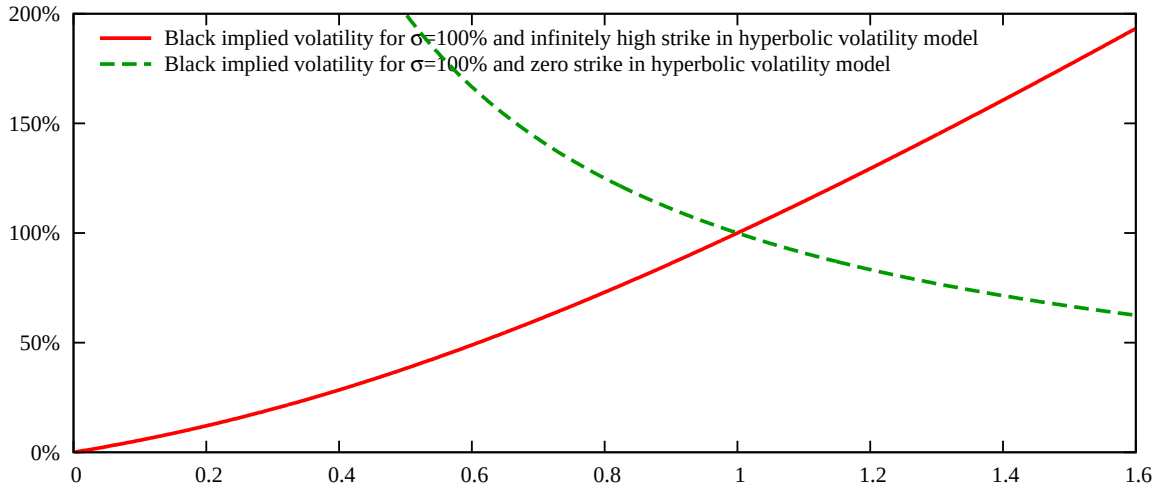

Figure 6: Black's implied volatility as given by the hyperbolic local volatlity model in the limit of infinitely high strike and zero strike as a function of β assuming that $\sigma = 1$ in equation (10) and $\zeta(x) = h(x)$ as defined in (22). The curves shown are the functional forms (23) and (24).

are governed by the parametric local volatility model (10) is given by

$$
\begin{aligned}
\hat{\sigma} \;=\; & \sigma + \tfrac{1}{2}\sigma\xi\,(\zeta_1 - 1) \\
& + \tfrac{1}{24}\sigma\Big[\sigma^2 T\,[1 - \zeta_1^2 + 2\zeta_2] + \xi^2\,[-2\zeta_1\,(3+\zeta_1) + 4\,(2+\zeta_2)]\Big] \\
& + \tfrac{1}{48}\sigma\Big[\sigma^2 T\xi\,[(\zeta_1-1)(3-\zeta_1^2+2\zeta_2) + 2\zeta_3] \\
& \qquad + 2\xi^3\,[-6 + \zeta_1\,(4+\zeta_1+\zeta_1^2-2\zeta_2) - 2\zeta_2 + \zeta_3]\Big] \\
& + \tfrac{1}{5760}\sigma\Big[3\sigma^4 T^2\,[7 + 3\zeta_1^4 + 4(5+3\zeta_2)\zeta_2 - 2\zeta_1^2(5+6\zeta_2) + 16\zeta_1\zeta_3 + 8\zeta_4] \\
& \qquad + 2\sigma^2 T\xi^2\,[209 + 30\zeta_1^3 + 11\zeta_1^4 + \zeta_1^2(20-44\zeta_2) \\
& \qquad\qquad + 4\zeta_2(35+11\zeta_2) - 6\zeta_1(45+10\zeta_2-12\zeta_3) - 60\zeta_3 + 36\zeta_4] \\
& \qquad - 8\xi^4\,[15\zeta_1^3 + 19\zeta_1^4 + \zeta_1^2(20-46\zeta_2) + 8\zeta_2(-5+2\zeta_2) \\
& \qquad\qquad + \zeta_1(-30\zeta_2 + 18(5+\zeta_3)) + 3(5\zeta_3 - 2(24+\zeta_4))]\Big] \\
& + \mathcal{O}(\sigma^7 T^3) + \mathcal{O}(\sigma^5 T^2\xi) + \mathcal{O}(\sigma^3 T\xi^3) + \mathcal{O}(\sigma\xi^5)
\end{aligned}
\tag{25}
$$

wherein

$$\zeta_1 = \zeta'(1) \quad \zeta_2 = \zeta''(1) \quad \zeta_3 = \zeta'''(1) \quad \zeta_4 = \zeta''''(1)\,. \tag{26}$$

For the CEV model, with $\zeta(x) = x^\beta$, this gives the at-the-money expressions

$$\hat{\sigma}_{\text{CEV}}\big|_{\xi=0} \;=\; \sigma \cdot \left[1 + \frac{\sigma^2 T}{24}\,(1-\beta)^2 + \frac{\sigma^4 T^2}{1920}\,(1-\beta)^2\left(7 - 54\beta + 27\beta^2\right) + \mathcal{O}(\sigma^6 T^3)\right] \tag{27}$$

$$\left.\frac{\mathrm{d}\hat{\sigma}_{\text{CEV}}}{\mathrm{d}\xi}\right|_{\xi=0} \;=\; \frac{1}{2}\sigma(\beta-1)\cdot\left[1 + \frac{\sigma^2 T}{8}\,(1-\beta)^2 + \mathcal{O}(\sigma^4 T^2)\right]\,. \tag{28}$$

For the displaced diffusion model with $\zeta(x) = \beta x + 1 - \beta$, we obtain

$$\hat{\sigma}_{\text{DD}}\big|_{\xi=0} \;=\; \sigma \cdot \left[1 + \frac{\sigma^2 T}{24}\left(1-\beta^2\right) + \frac{\sigma^4 T^2}{1920}\left(7 - 10\beta^2 + 3\beta^4\right) + \mathcal{O}(\sigma^6 T^3)\right] \tag{29}$$

$$\left.\frac{\mathrm{d}\hat{\sigma}_{\text{DD}}}{\mathrm{d}\xi}\right|_{\xi=0} \;=\; \frac{1}{2}\sigma(\beta-1)\cdot\left[1 + \frac{\sigma^2 T}{24}\left(3-\beta^2\right) + \mathcal{O}(\sigma^4 T^2)\right]\,. \tag{30}$$

For the hyperbolic volatility model, we have

$$\begin{aligned} \zeta_1 &= \beta & \qquad \zeta_2 &= \beta(\beta-1) \\ \zeta_3 &= -3\beta(\beta-1) & \qquad \zeta_4 &= -3\beta(\beta-1)(\beta^2-4)\,, \end{aligned} \tag{31}$$

and thus

$$\begin{aligned} \hat{\sigma}_{\text{hyperbolic}} \;=\;& \sigma + \\ & \sigma \cdot \tfrac{\beta-1}{2} \cdot \Big(\tfrac{\sigma^2 T}{12}(\beta-1) - \tfrac{\sigma^4 T^2}{960}(7 - \beta(109 - 3\beta(19+7\beta))) + \mathcal{O}(\sigma^6 T^3) \\ & \quad + \xi \cdot \left[1 + \tfrac{\sigma^2 T}{24}\,(3 - \beta(8-\beta)) + \mathcal{O}(\sigma^4 T^2)\right] \\ & \quad + \xi^2 \cdot \left[\tfrac{1}{6}(\beta-4) - \tfrac{\sigma^2 T}{1440}\,(209 - \beta(813 - \beta(279 + 97\beta))) + \mathcal{O}(\sigma^4 T^2)\right] \\ & \quad + \xi^3 \cdot \left[\tfrac{1}{12}(6 - \beta(3+\beta)) + \mathcal{O}(\sigma^2 T)\right] \\ & \quad + \xi^4 \cdot \left[\tfrac{1}{360}(-144 + \beta(103 + \beta(66 - 7\beta))) + \mathcal{O}(\sigma^2 T)\right] \\ & \quad + \mathcal{O}(\xi^5)\Big)\,. \end{aligned} \tag{32}$$

Denoting log-moneyness as $\varkappa = \ln(1+\xi)$, i.e. $\xi = \mathrm{e}^\varkappa - 1$, and expanding (32) in $\varkappa$ around 0, we obtain within the same approximation order:

$$\begin{aligned} \hat{\sigma}_{\text{hyperbolic}} \;\approx\;& \sigma + \\ & \sigma \cdot \tfrac{\beta-1}{2} \cdot \Big(\tfrac{\sigma^2 T}{12}(\beta-1) - \tfrac{\sigma^4 T^2}{960}(7 - \beta(109 - 3\beta(19+7\beta))) \\ & \quad + \varkappa \cdot \left[1 + \tfrac{\sigma^2 T}{24}\,(3 - \beta(8-\beta))\right] \\ & \quad + \varkappa^2 \cdot \left[\tfrac{1}{6}(\beta-1) - \tfrac{\sigma^2 T}{1440}\,(119 - \beta(573 - \beta(249 + 97\beta)))\right] \\ & \quad + \varkappa^3 \cdot \left[\tfrac{1}{12}(-\beta(1+\beta)) - \tfrac{\sigma^2 T}{1440}\,(179 - \beta(733 - \beta(269 + 97\beta)))\right] \\ & \quad + \varkappa^4 \cdot \Big[\tfrac{1}{360}(1 + \beta(3 + \beta(21 - 7\beta))) \\ & \qquad - \tfrac{\sigma^2 T}{17280}\,(1373 - \beta(5451 - \beta(1923 + 679\beta)))\Big]\Big)\,. \end{aligned} \tag{33}$$

Expansion (33) is a fourth order polynomial in log-moneyness. For strikes near the money, we expect it to be highly accurate. However, as strikes deviate from the money significantly, we expect it to perform increasingly badly since a fourth order polynomial for implied volatility is guaranteed to lead to arbitrage, i.e. negative risk-neutral densities far away from the money. In the following, we try to recast (33) such that near the money, we retain the accuracy as above, but as we move away from the money, we have a more reasonable behaviour than a fourth order polynomial. Our first step towards such an adjustment is to consider the behaviour of local volatility for small times to expiry.

It is possible to show generically by the aid of asymptotic expansions [BBF02] that for small times to expiry, local volatility models of the form (10) give rise to the following behaviour for implied volatility:

$$\lim_{T\to 0}\hat{\sigma} \;=\; \sigma\cdot\frac{\varkappa}{\left|\int_1^{\mathrm{e}^{\varkappa}}\frac{\mathrm{d}y}{\zeta(y)}\right|} \;=\; \sigma\cdot\frac{\varkappa}{\left|\int_0^{\varkappa}\frac{\mathrm{e}^{z}}{\zeta(\mathrm{e}^{z})}\mathrm{d}z\right|}\;. \tag{34}$$

In other words, implied volatility, in the limit of $T\to 0$, converges to the harmonic average of absolute local volatility on a logarithmic scale. For the hyperbolic local volatility model with $\zeta(x)=h(x)$ given in (22), the integral in (34) can be computed in closed form involving only elementary functions, though, we omit the rather lengthy resulting formula for the sake of brevity. More interesting than the exact expression is that it allows us to compute the asymptotics

$$\lim_{\varkappa\to-\infty}\lim_{T\to 0}\hat{\sigma}_{\text{hyperbolic}} \;=\; \frac{1}{\beta} \tag{35}$$

and

$$\begin{aligned}&\lim_{\varkappa\to-\infty}\lim_{T\to 0}\left((\hat{\sigma}_{\text{hyperbolic}}-1/\beta)\cdot\varkappa\right) \;=\\ &\frac{1}{2\beta^3}\cdot\left[2(1+\beta(\beta-1))\ln\beta+(\beta-1)\ln 4+2(\beta-1)\sqrt{1+\beta^2}\ln\left(\beta\frac{\sqrt{1+\beta^2}-\beta}{\sqrt{1+\beta^2}+1}\right)\right]\;.\end{aligned} \tag{36}$$

This means that for $\varkappa\to-\infty$, implied volatility for very short times to maturity behaves approximately like

$$\hat{\sigma}_{\text{hyperbolic}} \;\approx\; \sigma\cdot(1/\beta+c/\varkappa) \tag{37}$$

with c given by the right hand side of (36). In order to retain a similar asymptotic behaviour for all T, quartic polynomial behaviour near $\varkappa\approx 0$, and the limits (23) and (24), we assume for the functional form of implied volatility

$$\hat{\sigma}_{\text{hyperbolic}} \;=\; \sigma\cdot\frac{\sum_{j=0}^{4}c_j\varkappa^j}{1+\lambda|\varkappa|^5}+\frac{\sigma}{\beta}\cdot\frac{\lambda|\varkappa|^5}{1+\lambda|\varkappa|^5}\cdot\left(1+\mathbf{1}_{\{\varkappa>0\}}(\beta-1)\left(\beta+\sqrt{1+\beta^2}\right)\right)\;. \tag{38}$$

The coefficients c_0, c_1, c_2, c_3, and c_4 can be directly taken from (33):

$$c_0 \;=1+\frac{\beta-1}{2}\cdot\left(\frac{\sigma^2T}{12}(\beta-1)-\frac{\sigma^4T^2}{960}(7-\beta(109-3\beta(19+7\beta)))\right) \tag{39}$$

$$c_1 \;=\frac{\beta-1}{2}\cdot\left(1+\frac{\sigma^2T}{24}(3-\beta(8-\beta))\right) \tag{40}$$

$$c_2 \;=\frac{\beta-1}{12}\cdot\left(\beta-1-\frac{\sigma^2T}{240}(119-\beta(573-\beta(249+97\beta)))\right) \tag{41}$$

$$c_3 \;=\frac{1-\beta}{24}\cdot\left(\beta(\beta+1)+\frac{\sigma^2T}{120}(179-\beta(733-\beta(269+97\beta)))\right) \tag{42}$$

$$c_4 \;=\frac{\beta-1}{34560}\cdot\left(48(1+\beta(3+7\beta(3-\beta)))-\sigma^2T(1373-\beta(5451-\beta(1923+679\beta)))\right) \tag{43}$$

In order to determine the unknown coefficient λ, we demand that $\hat{\sigma}$ behaves like (37) for low strikes[1], i.e. for $\varkappa \to -\infty$. This yields

$$\lambda = \frac{\beta^3(1-\beta)(1+\beta(3+7\beta(3-\beta)))}{360\left[2(1+\beta(\beta-1))\ln\beta+(\beta-1)\ln 4+2(\beta-1)\sqrt{1+\beta^2}\ln\left(\beta\frac{\sqrt{1+\beta^2}-\beta}{\sqrt{1+\beta^2}+1}\right)\right]}. \tag{44}$$

4 Numerical comparison

We show in figures 7 to 16 a comparison between numerical results obtained with a finite difference solver and the analytical approximation (38) for a variety of parameter combinations.

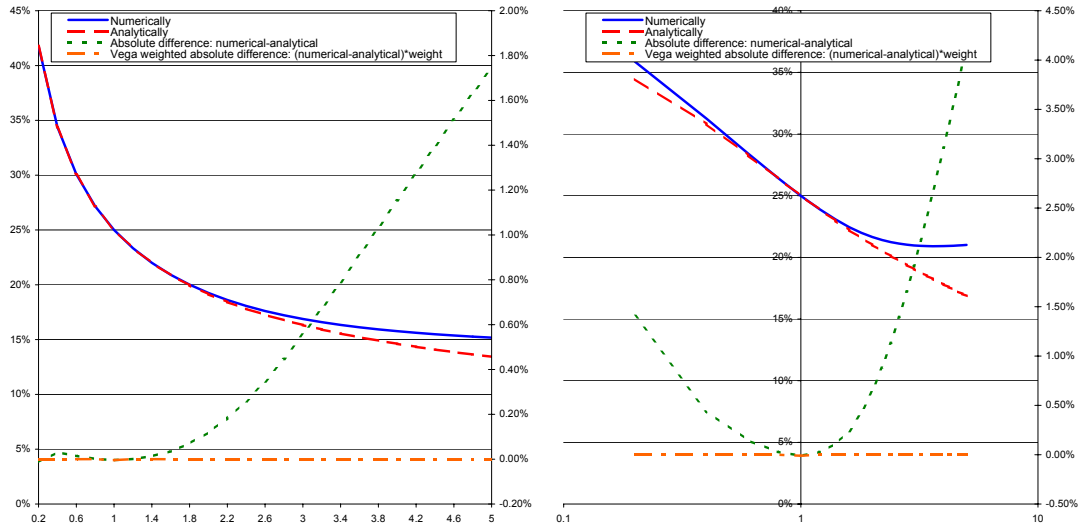

Figure 7: Numerical and analytically obtained implied volatility values for the hyperbolic volatility model for $T = 1/12$, $\sigma = 1/4$, $\beta = 1/2$ on linear (left) and logarithmic (right) strike scale. Error values are scaled along the right axes.

[1]The reason we choose the left hand side asymptotic behaviour is given by the financial observation that low strikes are typically of significantly greater interest in the market than very high strikes.

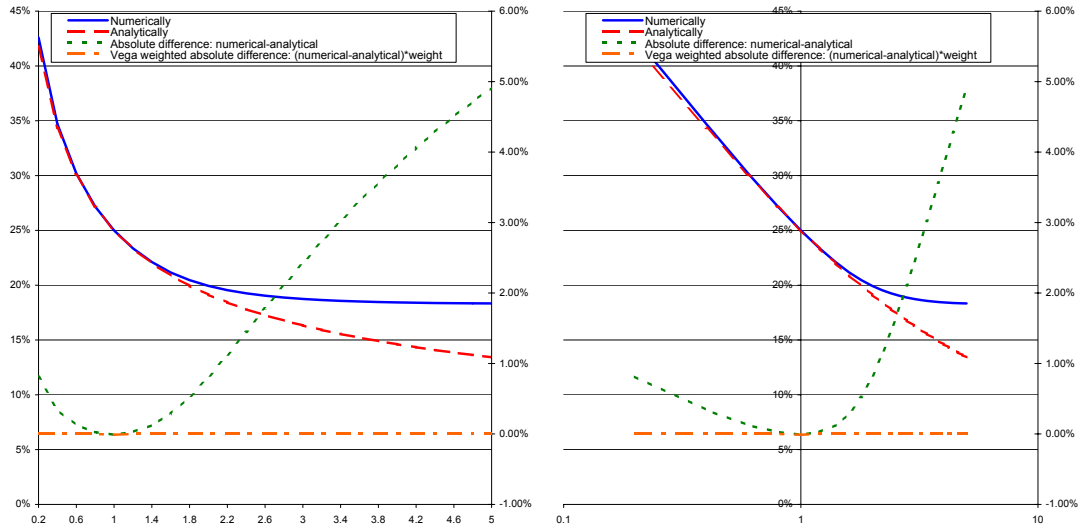

Figure 8: Numerical and analytically obtained implied volatility values for the hyperbolic volatility model for $T = 1/12$, $\sigma = 1/4$, $\beta = 1/4$ on linear (left) and logarithmic (right) strike scale. Error values are scaled along the right axes.

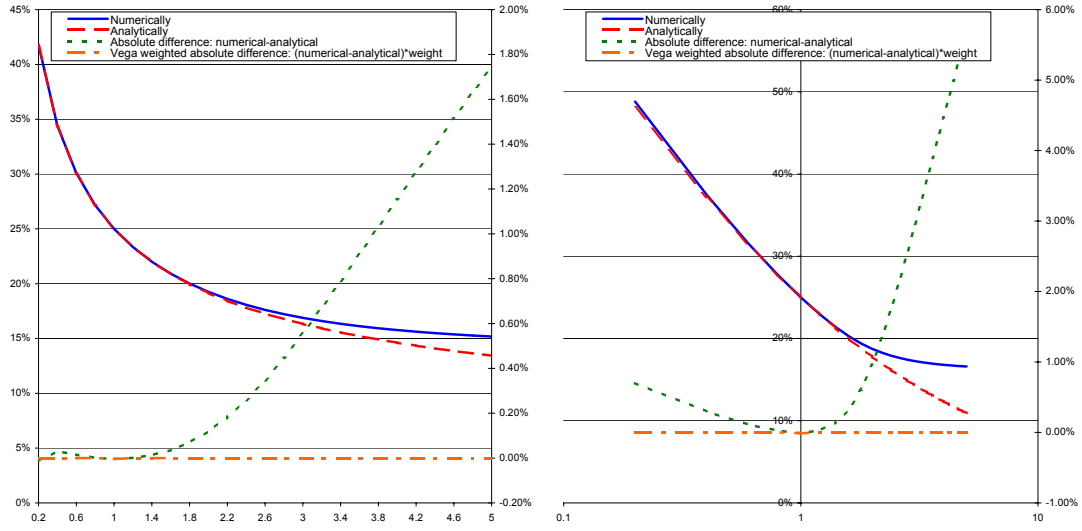

Figure 9: Numerical and analytically obtained implied volatility values for the hyperbolic volatility model for $T = 1/12$, $\sigma = 1/4$, $\beta = 1/16$ on linear (left) and logarithmic (right) strike scale. Error values are scaled along the right axes.

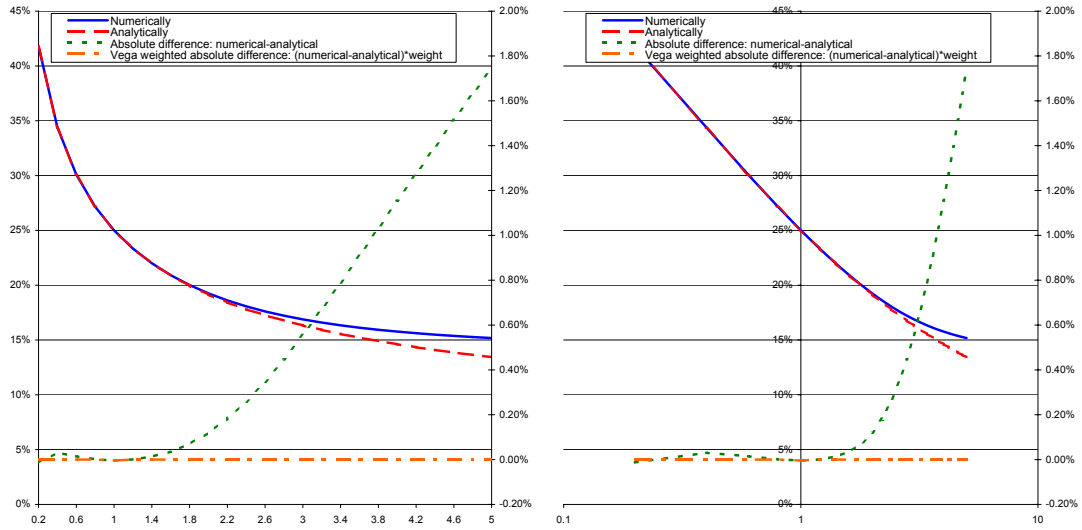

Figure 10: Numerical and analytically obtained implied volatility values for the hyperbolic volatility model for $T = 1/4$, $\sigma = 1/4$, $\beta = 1/4$ on linear (left) and logarithmic (right) strike scale. Error values are scaled along the right axes.

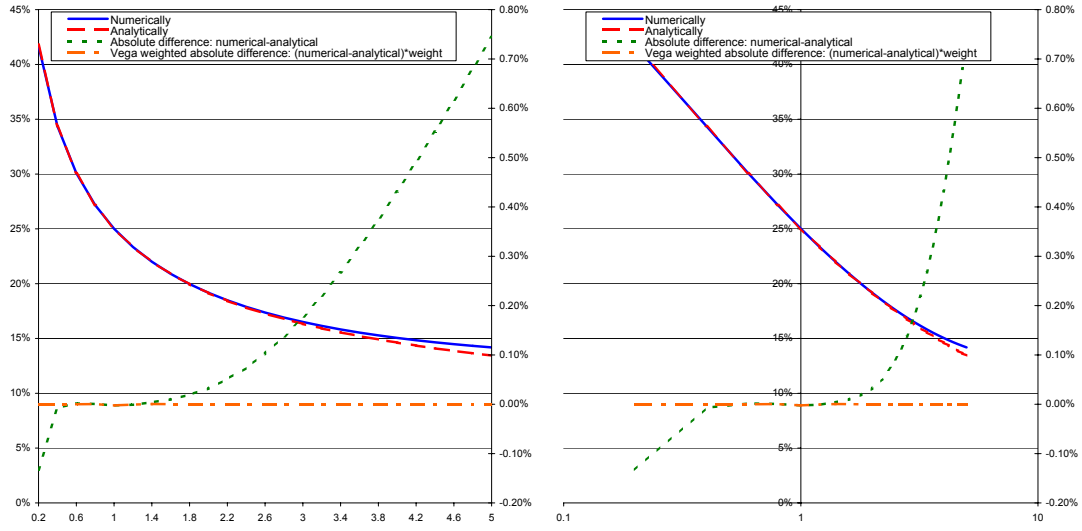

Figure 11: Numerical and analytically obtained implied volatility values for the hyperbolic volatility model for $T = 1/2$, $\sigma = 1/4$, $\beta = 1/4$ on linear (left) and logarithmic (right) strike scale. Error values are scaled along the right axes.

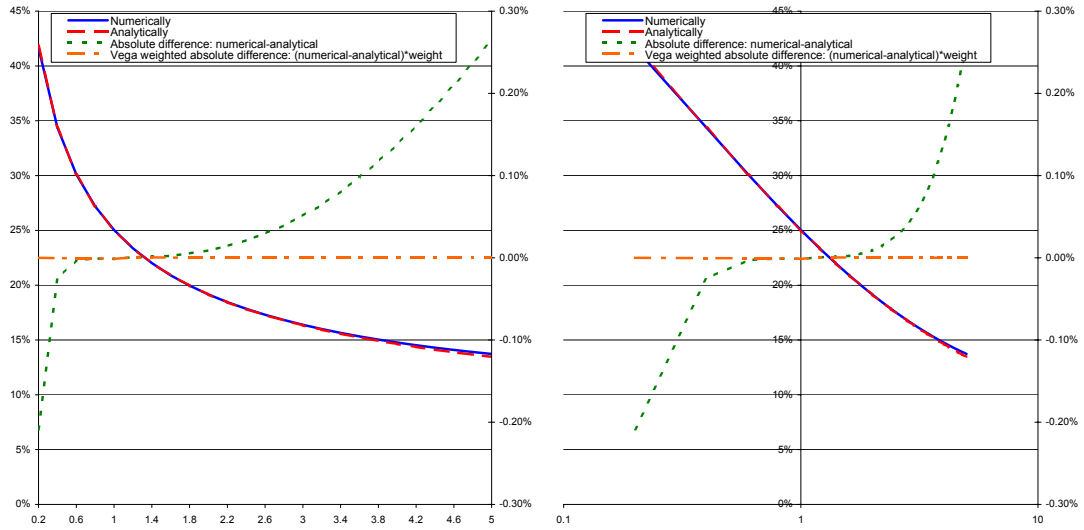

Figure 12: Numerical and analytically obtained implied volatility values for the hyperbolic volatility model for $T = 1$, $\sigma = 1/4$, $\beta = 1/4$ on linear (left) and logarithmic (right) strike scale. Error values are scaled along the right axes.

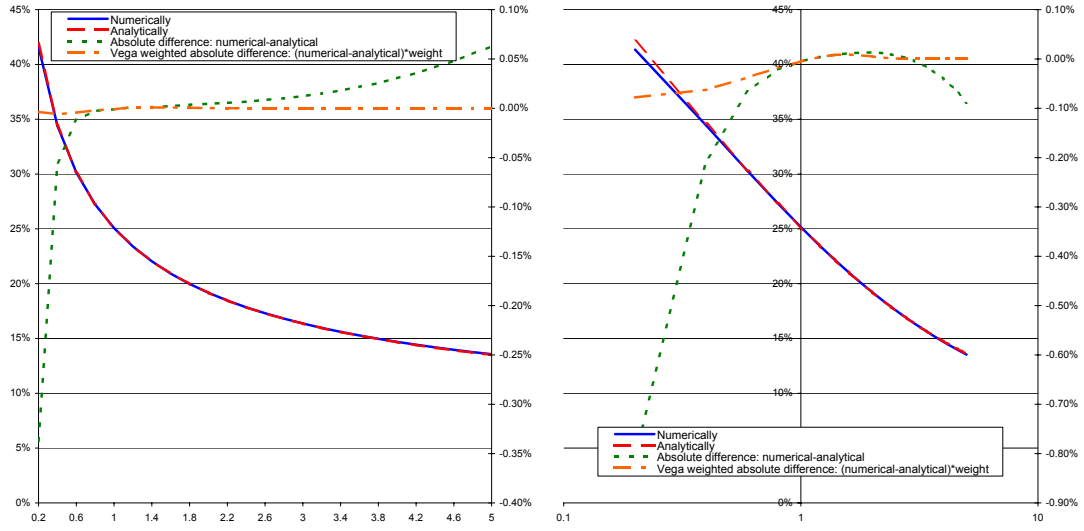

Figure 13: Numerical and analytically obtained implied volatility values for the hyperbolic volatility model for $T = 2$, $\sigma = 1/4$, $\beta = 1/4$ on linear (left) and logarithmic (right) strike scale. Error values are scaled along the right axes.

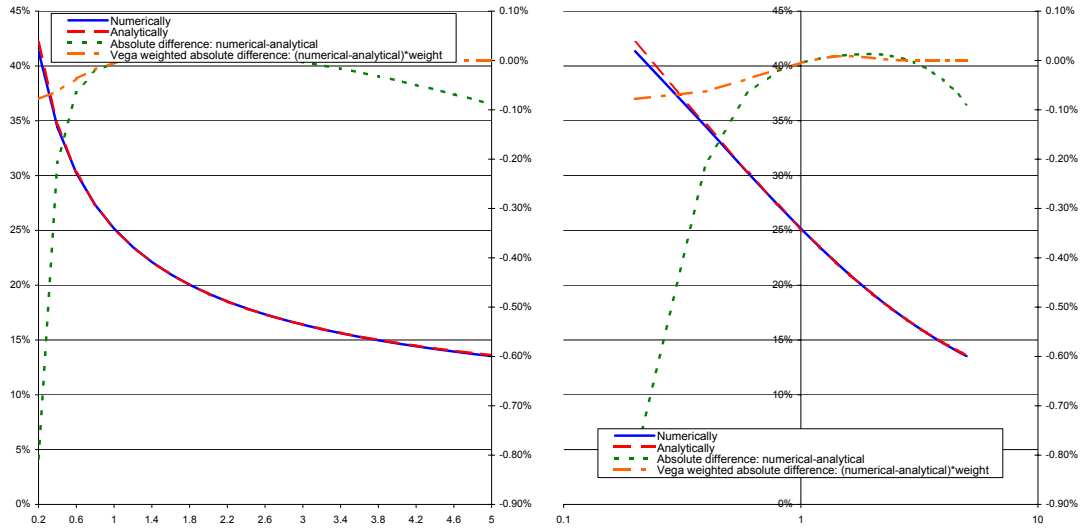

Figure 14: Numerical and analytically obtained implied volatility values for the hyperbolic volatility model for $T = 5$, $\sigma = 1/4$, $\beta = 1/4$ on linear (left) and logarithmic (right) strike scale. Error values are scaled along the right axes.

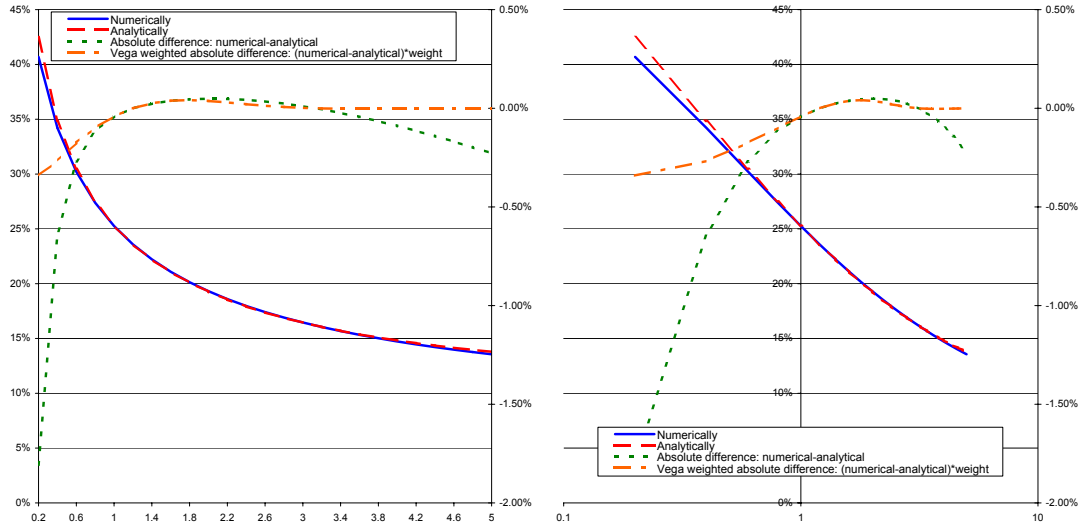

Figure 15: Numerical and analytically obtained implied volatility values for the hyperbolic volatility model for $T = 10$, $\sigma = 1/4$, $\beta = 1/4$ on linear (left) and logarithmic (right) strike scale. Error values are scaled along the right axes.

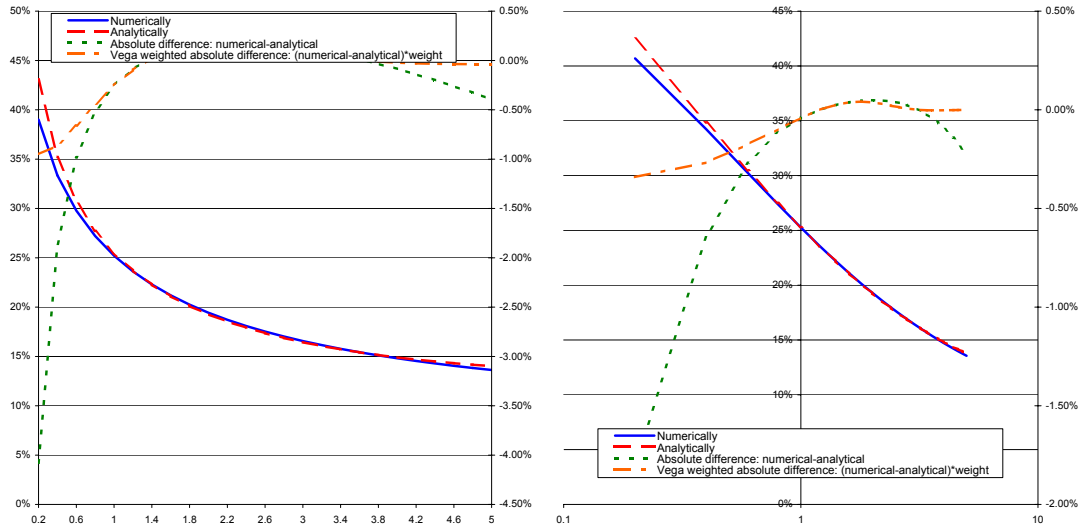

Figure 16: Numerical and analytically obtained implied volatility values for the hyperbolic volatility model for $T = 20$, $\sigma = 1/4$, $\beta = 1/4$ on linear (left) and logarithmic (right) strike scale. Error values are scaled along the right axes.

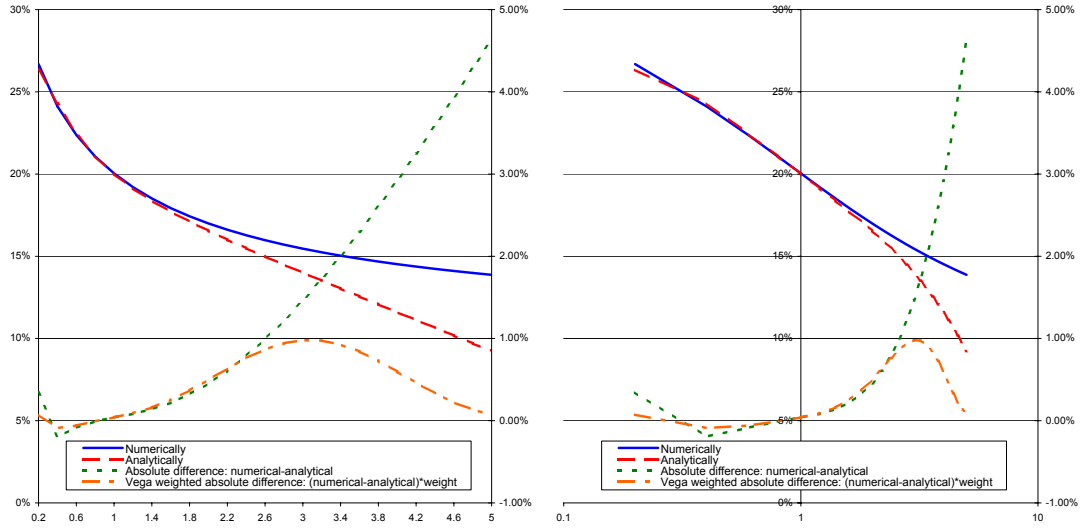

Figure 17: Numerical and analytically obtained implied volatility values for the hyperbolic volatility model for $T = 30$, $\sigma = 1/5$, $\beta = 1/2$ on linear (left) and logarithmic (right) strike scale. Error values are scaled along the right axes.

References

[AA00] L. Andersen and J. Andreasen. Volatility Skews and Extensions of the Libor Market Model. *Applied Mathematical Finance*, 7(1):1–32, March 2000.

[BBF02] H. Berestycki, J. Busca, and I. Florent. Asymptotics and calibration of local volatility models. *Quantitative Finance*, 2:61–69, 2002. www.iop.org/EJ/article/1469-7688/2/1/305/qf2105.pdf.

[Bec80] S. Beckers. The constant elasticity of variance model and its implications for option pricing. *Journal of Finance*, XXXV(3):661–673, June 1980.

[Cox75] J. C. Cox. Notes on option pricing I: Constant elasticity of variance diffusions. Working paper, Stanford University, 1975.

[Kah07] C. Kahl. *Modeling and simulation of stochastic volatility in finance*. PhD thesis, Bergische Universität Wuppertal and ABN AMRO, 2007. Published by www.dissertation.com, www.amazon.com/Modelling-Simulation-Stochastic-Volatility-Finance/dp/1581123833/, ISBN-10: 1581123833.

[NN05] Tomer Neu-Ner. An Effective Binomial Tree Algorithm for the CEV Model. Technical report, School of Computational and Applied Mathematics, University of the Witwatersrand, November 2005. www.cam.wits.ac.za/mfinance/projects/tomerneuner.pdf.

[Rub83] M. Rubinstein. Displaced diffusion option pricing. *Journal of Finance*, 38:213–217, March 1983.

[Sch89] M. Schroder. Computing the Constant Elasticity of Variance Option Pricing Formula. *Journal of Finance*, 44(1):211–219, March 1989. home.ust.hk/jinzhang/ust/Schroder_JF.pdf.

[Wat87] S. Watanabe. Analysis of Wiener functionals (Malliavin calculus) and its application to heat kernels. *The Annals of Probability*, 15:1–39, 1987.